The Journal of Open Source Software

MieSimulatorGUI: A user-friendly tool to compute and visualize light scattering by spherical dielectric particles

Janaka C. Ranasinghesagara [1,2], **Carole K. Hayakawa** [1,2], **Lisa M. Glover** [2], **and Vasan Venugopalan** [1,2¶]

1 Department of Chemical and Biomolecular Engineering, University of California, Irvine, California 92697, United States **2** Beckman Laser Institute and Medical Clinic, University of California, Irvine, California 92697, United States ¶ Corresponding author

DOI: 10.21105/joss.09551

Software

- Review
- Repository
- Archive

Editor: Henrik Finsberg

Reviewers:

- @MartinPdeS
- @GiannakopoulosIlias
- @ayusmin

Submitted: 08 July 2025
Published: 11 February 2026

Summary

Mie theory is a mathematical framework derived from Maxwell's equations that models electromagnetic scattering by spherical dielectric particles. Its predictions are essential across various scientific and engineering disciplines, including biomedical optics, atmospheric optics, particle characterization, nanofluids, computer graphics, and remote sensing. We developed `MieSimulatorGUI` to bridge the gap for researchers who require Mie simulations but lack specialized programming expertise. By integrating a high-performance C/C++ computational engine with the Qt framework, this user-friendly cross-platform tool calculates key optical properties such as scattering coefficients, cross-sections, angular scattering distributions, and scattering asymmetry for both monodisperse and polydisperse particle distributions. The graphical user interface (GUI) features six interactive panels that allow users to specify optical and particle input parameters, visualize particle distributions, and compute scattering metrics. Furthermore, it enables the fitting of the spectral dependence of the reduced scattering coefficient, a feature particularly valuable in fields like tissue optics. Licensed under MIT, `MieSimulatorGUI` is an open-source project hosted on GitHub and accessible via its download page.

Statement of need

Mie theory is derived from Maxwell's equations and provides a comprehensive framework for modeling electromagnetic scattering by spherical particles (Horvath, 2009; Mie, 1908). Mie theory is utilized across diverse fields, ranging from nanomaterials and biomedical optics to atmospheric science and astronomy (Bhandari et al., 2011; Chalut et al., 2008; Goody & Yung, 1995; Saidi et al., 1995; Wang et al., 2005). Despite its broad applicability, the theory's reliance on complex mathematical constructs, such as infinite series and special functions (Bohren & Huffman, 1983; Majic & Le Ru, 2020; van de Hulst, 1957; Wiscombe, 1980), demands advanced computational implementation.

While numerous Mie simulation packages are available (many of which are listed on SCATTPORT.org and Wikipedia), they generally fall into two categories: older, established codes focusing on computational efficiency (Bohren & Huffman, 1983; Wiscombe, 1980), and newer, object-oriented libraries typically hosted on version-control platforms (de Sivry-Houle et al., 2023; Giannakopoulos, Ilias, 2018; Prahl, 2023; Sumlin et al., 2018). Although both categories provide robust computational engines, they usually demand significant programming proficiency. This requirement creates a barrier for experimentalists, clinical scientists, and educators who need these analytical capabilities but may lack the specialized coding expertise to integrate such libraries into their workflows.

`MieSimulatorGUI` bridges this gap by providing an intuitive, cross-platform desktop application that computes and fits scattering parameters for monodisperse and polydisperse distributions without any coding. Unlike standard implementations, it supports heterogeneous polydispersity, allowing users to assign bin-specific complex refractive indices via custom data inputs, a feature often absent in simplified GUI tools. The tool facilitates high-impact use cases such as biomedical optics (Jacques, 2013; Mourant et al., 1997; Wang et al., 2005) and atmospheric research (Seinfeld & Pandis, 1997; Teri et al., 2022), where users can define complex particle configurations and directly fit spectrally-varying reduced scattering coefficients. By integrating a powerful C/C++ computational engine with intuitive Qt interface, `MieSimulatorGUI` offers accessible, yet powerful Mie theory computations, facilitating both streamlined research analysis and interactive pedagogical demonstrations.

Main Features

Built on the BHMIE (Bohren & Huffman, 1983) and Wiscombe (Wiscombe, 1979) frameworks, `MieSimulatorGUI` calculates spectral optical properties, including scattering coefficients, cross-sections, scattering amplitude matrix entries (S_1, S_2), phase functions, and scattering asymmetry. The tool supports both monodisperse and polydisperse particle distributions (Gélébart et al., 1996) and facilitates parameter estimation by fitting reduced scattering coefficient curves, a technique of significant value in tissue optics (Jacques, 2013). To ensure computational accuracy and GUI stability, the software includes an automated test suite integrated via GitHub Actions. Its high-performance C++ engine enables near-instantaneous computation and plotting, providing real-time visual updates across the spectral range. Comprehensive documentation, including cross-platform installation guides (Windows, Linux, and macOS), dependency specifications, command-line test execution, scattering regime analysis for dependent scattering, and several examples, is available on the Mie Simulator GUI Wiki page.

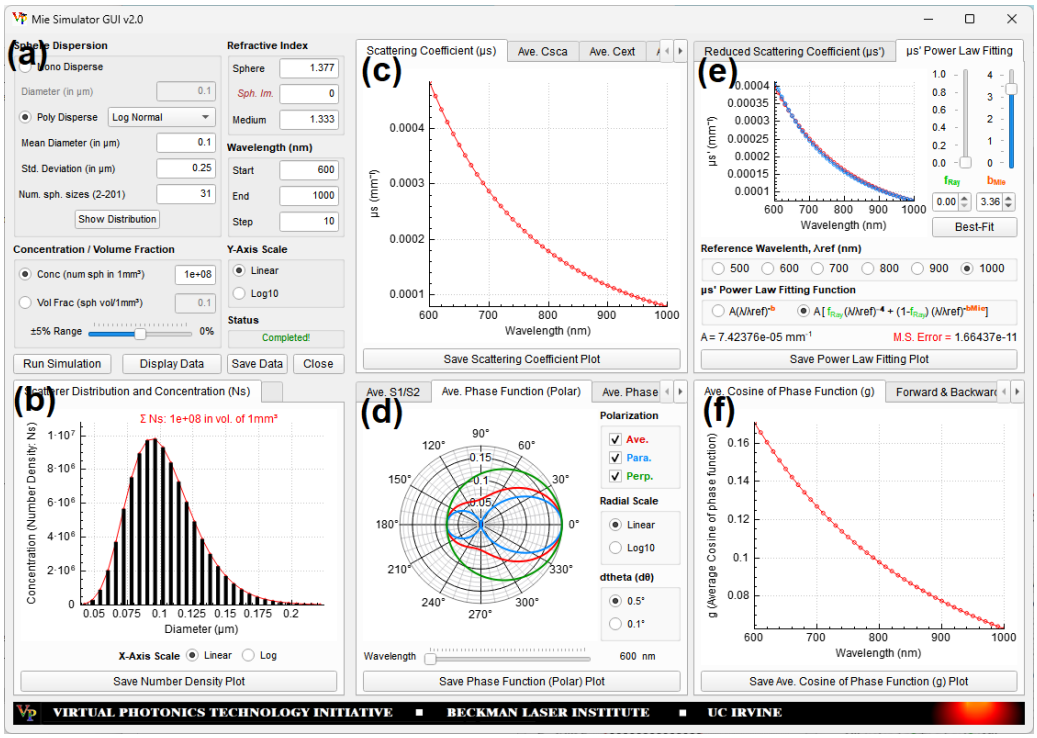

Figure 1: Six interactive panels of `MieSimulatorGUI`: (a) Input selection, (b) Particle size distribution, (c) Scattering coefficient, (d) Phase function, (e) Reduced Scattering, and (f) Scattering Asymmetry (Anisotropy)

Design and Functionality

The tool is distributed as portable binaries for Windows, macOS, and Linux. For local compilation, the project utilizes `qmake`, with dependencies (`Qt6` and `QCustomPlot`) managed via an automated build script. The Qt GUI contains six interactive panels (Figure 1).

Input Selection Panel

This panel enables the user to define inputs for Mie simulations at either a single wavelength or across a spectral range. The distribution of spheres is described using sphere concentration (`Conc`) (spheres/mm^3) or volume fraction (`Vol Frac`). The volume fraction represents the ratio of the volume occupied by the spherical particles to the total solution volume. For polydisperse systems, `Vol Frac` is calculated by multiplying the volume of each sphere size with its corresponding concentration per unit volume, and then summing across all sphere sizes. `MieSimulatorGUI` utilizes the independent scattering approximation, a framework valid for dilute suspensions where particles are sufficiently separated to ignore coherent interactions (Schmitt & Kumar, 1998; van de Hulst, 1957). The accuracy of this approximation decreases as volume fraction increases, as it is sensitive to `Size Parameter` and the ratio of particle spacing to wavelength (Galy et al., 2020; Tien & Drolen, 1987; Yalcin et al., 2022). Consequently, the tool is best suited for dilute systems and the results obtained for concentrated regimes may deviate from physical reality and should be interpreted with caution. Starting with `MieSimulatorGUI v2.0`, the tool triggers a warning if the inputs exceed the limits of independent scattering.

To maintain numerical stability in the BHMIE algorithm and ensure UI responsiveness, sphere diameters are restricted to a range of 0.1 nm to 300 µm, while wavelengths are limited to 50 nm – 3000 nm. These ranges cover the primary biomedical and atmospheric spectral windows. For absorbing spheres, the complex refractive index (m_{sphere}) is defined as m_{real} – j m_{imag}, where m_{real} and m_{imag} represent real and imaginary components, respectively (van de Hulst, 1957; Wiscombe, 1979).

The tool provides options for either monodisperse (uniform-sized) or polydisperse (variable-sized) particle distributions. Monodisperse distributions restrict analysis to spheres with uniform size and refractive index. In contrast, polydisperse distributions enable simulations of spheres with diverse attributes and support three size distribution models: 1. `Log-normal`, 2. `Gaussian`, and 3. `Custom` (user-defined). The `Custom` option allows for the specification of different refractive indices for different spheres, as demonstrated in the examples provided in the `CustomDataSamples` folder.

Number Density Panel

This panel graphically presents the number density of spheres N_s [#/ mm^3] used in the simulation. The subsequent tab displays the `Size Parameter` defined as $2\pi R n_{med}/\lambda_{vacuum}$ (Bohren & Huffman, 1983), where R [µm] denotes the particle radius, n_{med} the medium's refractive index, and λ_{vacuum} [µm] is the wavelength in vacuum.

Scattering Coefficient Panel

The Mie calculations provide three important efficiency factors: the scattering efficiency (Q_{sca}), the extinction efficiency (Q_{ext}), and the backscattering efficiency (Q_{back}). These dimensionless quantities combined with the particle's cross sectional area (πR^2) yield the corresponding scattering cross section C_{sca} [/mm^2], extinction cross section C_{ext} [/mm^2] and backscattering cross section C_{back} [/mm^2] (Bohren & Huffman, 1983; van de Hulst, 1957). The calculated cross sections are displayed across three separate tabs. For monodisperse distribution, the scattering coefficient (μ_s) is simply the product of the scattering cross-section C_{sca} and the number density N_s. For polydisperse distributions, the scattering coefficient is

computed via a discrete summation of the cross-sections across individual particle size bins, as detailed by Schmitt and Kumar (Schmitt & Kumar, 1998).

Phase Function Panel

The phase function represents the angular distribution of scattered light. The calculated phase function results are displayed in this panel using both polar and linear plots. These plots are derived from the complex amplitude scattering matrix elements, S_1, and S_2, which describe the transformation of incident electromagnetic field to far-field scattered field (Bohren & Huffman, 1983; van de Hulst, 1957). The wavelength slider allows the user to visualize the phase function or S_1 and S_2 data at any specific wavelength.

Scattering Asymmetry Panel

The scattering asymmetry (Anisotropy) panel displays the directional properties of the scattering phase function. The first tab presents the average cosine of the single scattering phase function (g), which quantifies the prevalence of forward ($g > 0$) vs backward scattering ($g < 0$). The second tab provides the integrated forward and backward scattering fractions, offering a detailed analysis of the angular scattering distribution.

Reduced Scattering Panel

This panel shows the reduced scattering coefficient (μ_s'), which is computed as the product of the scattering coefficient (μ_s) and $(1 - g)$ (Jacques, 2013). This parameter of particular interest in biomedical optics, as it enables the non-invasive quantification of tissue properties. Users can use μ_s' `Power Law Fitting` tab to compute the fitting parameters that provide a simplified functional form for the wavelength dependence of μ_s' (Jacques, 2013).

Example Application: Scattering of Intralipid Phantoms

To demonstrate the tool's scientific utility, we considered the characterization of Intralipid, a standard tissue phantom in biomedical optics (Di Ninni et al., 2011; van Staveren et al., 1991). Based on Intralipid particle distribution profiles in the literature (Kodach et al., 2011; Raju & Unni, 2017), we assumed a polydisperse `Log Normal` particle distribution with a mean diameter of 0.22 µm and a standard deviation of 0.37 µm. We set the refractive indices to 1.47 for the soybean oil droplets and 1.33 for the surrounding medium, while assigning a value of 101 to the `Num. sph. sizes` field. To analyze different concentrations ranging from 0.2% to 20% (Aernouts et al., 2013; van Staveren et al., 1991), volume fractions were scaled using a baseline value of 0.227 for a 20% (w/w) Intralipid concentration (Aernouts et al., 2013). Upon executing the simulation across the 400–2250 nm spectral range, `MieSimulatorGUI` calculates μ_s, μ_s' and g. While the selected volume fractions may exceed independent scattering limits established in the literature (Galy et al., 2020; Tien & Drolen, 1987; Yalcin et al., 2022), the results show strong agreement with established bulk scattering properties (Aernouts et al., 2013; van Staveren et al., 1991). Figures can be exported as `.png` files and results as text files for further analysis. Beyond preset distributions, the `Custom` option can be utilized to upload specific Intralipid sphere profiles (Raju & Unni, 2017).

Acknowledgments

We acknowledge support from the Laser Microbeam and Medical Program (LAMMP), a NIH Biomedical Technology Resource (P41-EB015890). JCR and VV acknowledge the support from the NIH (R21-GM128135) and the NSF (CBET-1805082). JCR was the primary contributor, handling the core software development, UI design, validation, GitHub upload, and drafting the original manuscript. VV provided overall supervision and critically reviewed and edited the

final manuscript. CKH developed the initial Mie scattering code, and LMG assisted with the GitHub and Zenodo uploads.

References

Aernouts, B., Zamora-Rojas, E., Beers, R. V., Watté, R., Wang, L., Tsuta, M., Lammertyn, J., & Saeys, W. (2013). Supercontinuum laser based optical characterization of intralipid® phantoms in the 500-2250 nm range. *Opt. Express*, *21*(26), 32450–32467.

Bhandari, A., Hamre, B., Frette, Ø., Stamnes, K., & Stamnes, J. J. (2011). Modeling optical properties of human skin using mie theory for particles with different size distributions and refractive indices. *Opt. Express*, *19*(15), 14549–14567. https://doi.org/10.1364/OE.19.014549

Bohren, C. F., & Huffman, D. R. (1983). *Absorption and Scattering of Light by Small Particles*. John Wiley; Sons, Inc. ISBN: 047105772X

Chalut, K. J., Giacomelli, M. G., & Wax, A. (2008). Application of mie theory to assess structure of spheroidal scattering in backscattering geometries. *J Opt Soc Am A*, *25*(8), 1866–1874. https://doi.org/10.1364/josaa.25.001866

de Sivry-Houle, M. P., Godbout, N., & Boudoux, C. (2023). PyMieSim: An open-source library for fast and flexible far-field mie scattering simulations. *Opt. Continuum*, *2*(3), 520–534. https://doi.org/10.1364/OPTCON.473102

Di Ninni, P., Martelli, F., & Zaccanti, G. (2011). Intralipid: towards a diffusive reference standard for optical tissue phantoms. *Phys. Med. Biol.*, *56*(2), N21–N28. https://doi.org/10.1088/0031-9155/56/2/N01

Galy, T., Huang, D., & Pilon, L. (2020). Revisiting independent versus dependent scattering regimes in suspensions or aggregates of spherical particles. *J. Quant. Spectrosc. Radiat. Transfer*, *246*, 106924. https://doi.org/10.1016/j.jqsrt.2020.106924

Gélébart, B., Tinet, E., Tualle, J. M., & Avrillier, S. (1996). Phase function simulation in tissue phantoms: a fractal approach. *Pure and Appl. Opt.*, *5*(4), 377–388. https://doi.org/10.1088/0963-9659/5/4/005

Giannakopoulos, Ilias. (2018). *Matlab software for the Mie scattering of PEC and homogeneous spheres irradiated by a linearly polarized plane wave*. https://www.github.com/GiannakopoulosIlias/MieScattering

Goody, R. M., & Yung, Y. L. (1995). *Atmospheric Radiation: Theoretical Basis* (2nd Edition, p. 540). Oxford University Press. ISBN: 978-0195356106

Horvath, H. (2009). Light scattering: Mie and more – commemorating 100 years of mie's 1908 publication. *J. Quant. Spectrosc. Radiat. Transfer*, *110*(11), 783–786. https://doi.org/10.1016/j.jqsrt.2009.03.001

Jacques, S. L. (2013). Optical properties of biological tissues: a review. *Phys. Med. Biol.*, *58*(11), R37–R61. https://doi.org/10.1088/0031-9155/58/11/R37

Kodach, V. M., Faber, D. J., Marle, J. van, Leeuwen, T. G. van, & Kalkman, J. (2011). Determination of the scattering anisotropy with optical coherence tomography. *Opt. Express*, *19*(7), 6131–6140. https://doi.org/10.1364/OE.19.006131

Majic, M., & Le Ru, E. C. (2020). Numerically stable formulation of Mie theory for an emitter close to a sphere. *Appl. Opt.*, *59*(5), 1293–1300. https://doi.org/10.1364/ao.379694

Mie, G. (1908). Beiträge zur Optik trüber Medien, speziell kolloidaler Metallösungen. *Annalen Der Physik*, *330*(3), 377–445. https://doi.org/10.1002/andp.19083300302

Mourant, J. R., Fuselier, T., Boyer, J., Johnson, T. M., & Bigio, I. J. (1997). Predictions

and measurements of scattering and absorption over broad wavelength ranges in tissue phantoms. *Appl. Opt.*, *36*(4), 949–957. https://doi.org/10.1364/AO.36.000949

Prahl, S. (2023). *Mie scattering* (Version v2.6.3). https://doi.org/10.5281/zenodo.10087653

Raju, M., & Unni, S. N. (2017). Concentration-dependent correlated scattering properties of intralipid 20% dilutions. *Appl. Opt.*, *56*(4), 1157–1166. https://doi.org/10.1364/AO.56.001157

Saidi, I. S., Jacques, S. L., & Tittel, F. K. (1995). Mie and rayleigh modeling of visible-light scattering in neonatal skin. *Appl. Opt.*, *34*(31), 7410–7418. https://doi.org/10.1364/ao.34.007410

Schmitt, J. M., & Kumar, G. (1998). Optical scattering properties of soft tissue: A discrete particle model. *Appl. Opt.*, *37*(13), 2788–2797. https://doi.org/10.1364/AO.37.002788

Seinfeld, J. H., & Pandis, S. N. (1997). *Atmospheric chemistry and physics: Air pollution to climate change*. Wiley-Interscience. ISBN: 0471178160

Sumlin, B. J., Heinson, W. R., & Chakrabarty, R. K. (2018). Retrieving the aerosol complex refractive index using PyMieScatt: A mie computational package with visualization capabilities. *J. Quant. Spectrosc. Radiat. Transfer*, *205*, 127–134. https://doi.org/10.1016/j.jqsrt.2017.10.012

Teri, M., Müller, T., Gasteiger, J., Valentini, S., Horvath, H., Vecchi, R., Bauer, P., Walser, A., & Weinzierl, B. (2022). Impact of particle size, refractive index, and shape on the determination of the particle scattering coefficient – an optical closure study evaluating different nephelometer angular truncation and illumination corrections. *Atmosph. Meas. Tech.*, *15*(10), 3161–3187. https://doi.org/10.5194/amt-15-3161-2022

Tien, C. L., & Drolen, B. L. (1987). Thermal radiation in particulate media with dependent and independent scattering. *Annu. Rev. Heat Trans.*, *1*, 1–32. https://doi.org/10.1615/AnnualRevHeatTransfer.v1.30

van de Hulst, H. C. (1957). *Light scattering by small particles* (p. 470). John Wiley; Sons Inc.

van Staveren, H. J., Moes, C. J. M., Marle, J. van, Prahl, S. A., & Gemert, M. J. C. van. (1991). Light scattering in Intralipid-10% in the wavelength range of 400–1100 nm. *Appl. Opt.*, *30*(31), 4507–4514. https://doi.org/10.1364/ao.30.004507

Wang, X., Pogue, B. W., Jiang, S., Song, X., Paulsen, K. D., Kogel, C., Poplack, S. P., & Wells, W. A. (2005). Approximation of Mie scattering parameters in near-infrared tomography of normal breast tissue in vivo. *J Biomed. Opt.*, *10*(5), 051704. https://doi.org/10.1117/1.2098607

Wiscombe, W. J. (1979). *Mie Scattering Calculations : Advances in Technique and Fast, Vector-Speed Computer Codes* (NCAR/TN-140+STR). National Center for Atmospheric Research (NCAR). https://doi.org/10.5065/D6ZP4414

Wiscombe, W. J. (1980). Improved mie scattering algorithms. *Appl. Opt.*, *19*(9), 1505–1509. https://doi.org/10.1364/AO.19.001505

Yalcin, R. A., Lee, T., Kashanchi, G. Na., Markkanen, J., Martinez, R., Tolbert, S. H., & Pilon, L. (2022). Dependent scattering in thick and concentrated colloidal suspensions. *ACS Photonics*, *9*(10), 3318–3332. https://doi.org/10.1021/acsphotonics.2c00664